IET Science, Measurement & Technology

Research Article

IET Journals
The Institution of Engineering and Technology

Correction about rear of aperture serves as sphere wall in effective area method

ISSN 1751-8822
Received on 3rd July 2015
Revised on 11th September 2015
Accepted on 28th September 2015
doi: 10.1049/iet-smt.2015.0142
www.ietdl.org

Xiangzi Chen[1], Wei Fang[2], Shuyan Xu[2], Xiangqian Quan[1], Zhiwei Xia[2], Kai Wang[2], Yupeng Wang[2] ✉

[1]*Daheng College, University of Chinese Academy of Sciences, Beijing 100049, People's Republic of China*
[2]*The First Space Department, Fine Mechanics and Physics, Chinese Academy of Sciences, Changchun Institute of Optics, Changchun 130033, People's Republic of China*
✉ *E-mail: xzchen913@163.com*

Abstract: To eliminate the non-uniformity response of integrating sphere detector, which is brought by the back surface of the measured main aperture of the solar irradiance absolute radiometer serving as a part of the integrating sphere wall in effective area method, a correction optical model is designed to tackle the issue in TracePro program. By simulations, the radiant flux responded by the integrating sphere detector is given. Then the curve of the relative change about the radiant flux is deduced and the experiment measurement data are corrected on the basis of relative change curve. Eventually, the uncorrected and the corrected main aperture areas are calculated. Within a series of repeated measurements, the relative uncertainties of the uncorrected results and the corrected results are both 7×10^{-5} ($n = 7$). The relative uncertainty of the differences between the raw results and corrected results is 9.65×10^{-5} which proves that the optical model can evaluate the deviation, efficiently.

1 Introduction

As an important energy source to the earth, solar power promotes the circulation of the energy. Its effects on the climatic variation and environmental change are very significant. It is essential to measure and make a long-term monitoring about the solar irradiance. For this purpose, the solar irradiance absolute radiometer (SIAR) is researched and developed by Changchun Institute of Optics, Fine Mechanics and Physics, Chinese Academy of Sciences [1–7]. The solar constant monitor mounted on SZ-3 spacecraft and the solar total irradiance monitors boarded on the FY meteorological satellite are all composed by SIARs [8–12]. The SIAR is a kind of dual-conical cavity compensation absolute radiometer and there is a main aperture in front of the cavity. The main aperture is a type of knife edge circular aperture [13]. Its area determines the solid angle needed for the definition of radiant intensity, so it determines the measurement accuracy of the SIAR directly. We use the effective area method [14–17] to measure the main aperture of the SIAR. The measurement accuracy of this method is high and the calibration situation is similar to that during the actual use of the apertures [18–20].

In this paper, the effective-area method is introduced and the schematic diagram of the experiment measurement setup is shown first. Then a problem is put forward that the rear of the measured main aperture will serve as a part of integrating sphere wall during the process of the aperture area measurement, which will make the measurement results unreliable. In order to correct the aperture area results, an optical model based on the real measurement situation is designed and simulated in TracePro programs. Then the radiant fluxes detected by the sphere detector are recorded along with the different positions of the main aperture. The curve of the relative change of radiant fluxes is deduced. Eventually, the aperture areas are acquired after correcting the experiment measurement data. The relative uncertainty of the differences between the raw results and corrected results is given.

2 The effective-area method

The measured main aperture is placed in a known and uniform irradiance (E) light region in which the direction of the light propagation and the plane of the aperture are perpendicular. The total radiant flux passing through the aperture is P. The radio of the total radiant flux to the irradiance gives the measured main aperture area. The equation is

$$A = \frac{P}{E} \tag{1}$$

This uniform and known irradiance light region can be formed through fixing one laser Gaussian beam in which the radiant flux is P_L, moving the measured aperture by a x–y translation stage in constant step lengths (Δx and Δy), forming a regular grid of $(2n_x + 1) \times (2n_y + 1)$ in the x and y directions. A special detector should be designed to collect the entire radiant flux scattering out of the aperture edge, since the position of the aperture is changing. A combination of the integrating sphere and detector can solve this problem. The integrating sphere detector is placed behind the measured aperture to collect the radiant flux. When the stage carrying the aperture moves one step, the radiant flux is $P_{j,k}$. The total radiant flux passing the measured aperture is

$$P = \sum_{j=-n_x}^{n_x} \sum_{k=-n_y}^{n_y} P_{j,k} \tag{2}$$

The irradiance of the uniform light region is calculated by the equation

$$E = \frac{(2n_x + 1)(2n_y + 1)P_L}{(2n_x + 1)\Delta x(2n_y + 1)\Delta y} = \frac{P_L}{\Delta x \Delta y} \tag{3}$$

According to (1)–(3), the main aperture area can be calculated by the equation

$$A = \frac{P}{E} = \frac{\Delta x \Delta y \sum_{j=-n_x}^{n_x} \sum_{k=-n_y}^{n_y} P_{j,k}}{P_L} \tag{4}$$

The schematic diagram of the experiment measurement setup is shown in Fig. 1. The laser beam becomes a clean Gaussian beam

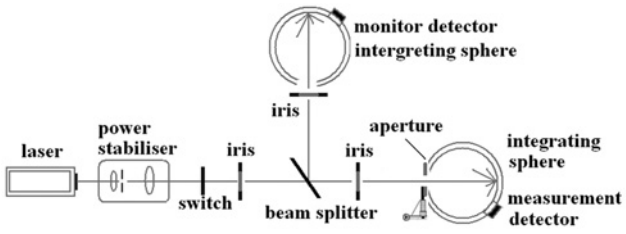

Fig. 1 *Schematic diagram of the experiment measurement setup*

with a power of about 2 mW after passing through the spatial filter and the power stabiliser with a type of Brockton Electro-Optics Laser Intensity Stabilizer (BEO LS-PRO). Over the time required for moving the measured aperture, the long-term instability about the power of Gaussian laser beam is about 3.0×10^{-5}. The Gaussian laser beam is divided into two beams after passing through the beam splitter. One beam reaches to the monitoring detector and the other reaches to the measurement detector. The monitoring detector is same as the measurement detector. They are all composed by a photo diode with a type of Hamamatsu S1227 and an integrating sphere. The integrating sphere is used to collect the scattering light which hits the knife edge of the aperture and spreads in a big solid angle. The monitoring detector is used to survey the stability of the laser beam power. Moreover, the measurement detector is used to measure the main aperture area. The main aperture is aligned perpendicularly to the measurement beam. The back surface of main aperture is near the input port (A) of the integrating sphere. When the two beams reach into the two integrating sphere detectors, the light signals become the electric signals which are detected by the two photo diodes connected to the multimeter with a type of Keighley 2700.

A problem existed that the back surface of the measured main aperture will serve as a part of the sphere wall during the measurement process. The non-uniformity in the reflectivity of the back surface might influence the radiant flux response by the sphere detector. Moreover, the main aperture area measurement results will be affected. A method should be found to evaluate and correct the effect.

3 Design of the optical model

An optical model should be designed to study the non-uniformity of the radiant flux responded by the sphere detector during the measurement process. An auxiliary beam could be introduced into the sphere detector by another input port to measure the relative changes of radiant flux with changing the position of the main aperture.

First, an optical model is designed in TracePro program which describes the original position of the laser beam, the measured main aperture, and the input port (A) of the integrating sphere detector during the real measurement situation. The optical model is shown in Fig. 2. The laser beam (measurement beam) comes into the integrating sphere through the input port (A) of the sphere detector, perpendicularly.

Second, another input port (B) and another laser beam (reference beam) are designed in the optical model additionally. The reference beam comes into the sphere detector through the input port (B). The area of the input port (B) is about the same size as the main aperture area. The reference beam is the same as the measurement beam except the spread direction. The measurement beam and reference beam come into the integrating sphere, and then hit the wall of the integrating sphere detector at the same position through the two input ports (A and B). The position of the input port (B) should be near the input port (A). The input port (B) with 12 different positions is designed in one side of the input port (A) which is shown in Fig. 3.

Finally, there are five situations that the distance between the measured main aperture and the input port (A) of the integrating sphere detector is 0, 0.75, 1, 1.25, and 1.5 mm. For each situation, we simulated the radiant flux responded by the integrating sphere detector with the 12 different positions of input port (B).

The radiant fluxes are recorded during the different situation simulations made in TracePro programs. The radiant flux responded by the integrating sphere detector is P_{m} when the measurement beam comes into the sphere. Moreover, the radiant flux responded by the integrating sphere detector is P_{r} when the reference beam comes into the sphere. After simulations, we study the differences between the recorded radiant fluxes. For each position of input (B), the relative change of the radiant flux is defined as $r = |P_{\mathrm{m}} - P_{\mathrm{r}}|/P_{\mathrm{m}}$. The curves of the relative change about the radiant fluxes responded by the integrating sphere detector are given, which are shown in Fig. 4.

On the basis of the curve, we found that the relative change of radiant flux (r) is the lowest when the input port (B) is in the position of 7. In our corrective optical model, the input port (B) is designed in position 7.

4 Corrective optical model

4.1 Process of the correction

The corrective optical model is shown in Fig. 5. The reference beam comes into the sphere through the input port (B). Moreover, the measurement beam does not come into the sphere. During the simulation process, the distance between the measured main aperture and the input port (A) of the integrating sphere is 1 mm. The aperture is scanned over the measurement area size of $(2n_x + 1)$ $(2n_y + 1)$ with constant step lengths. A radiant flux responded by the integrating sphere detector is recorded at every position.

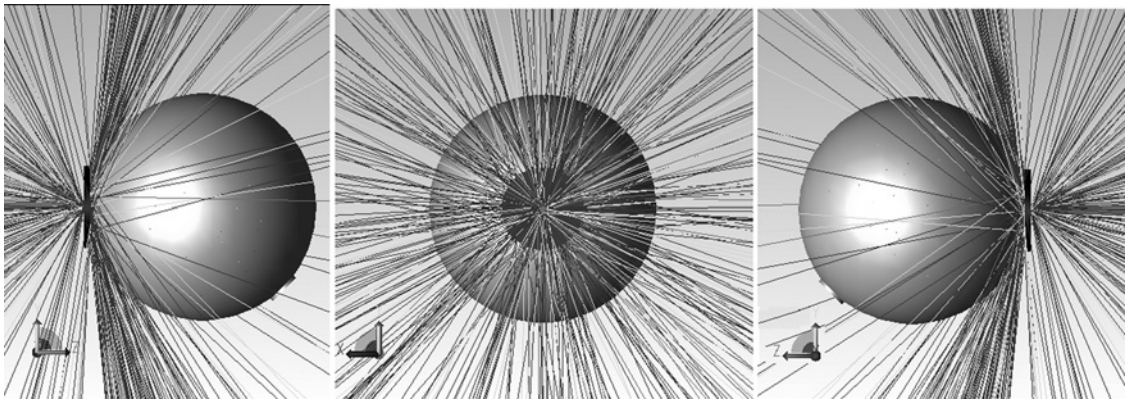

Fig. 2 *Optical model of the real measurement in different visual angles*

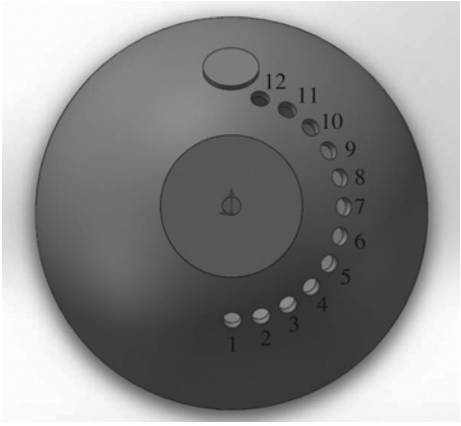

Fig. 3 *Input port B with different positions*

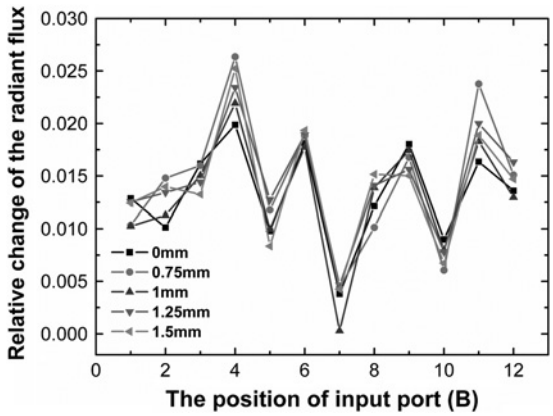

Fig. 4 *Curves of the relative change about the radiant flux*

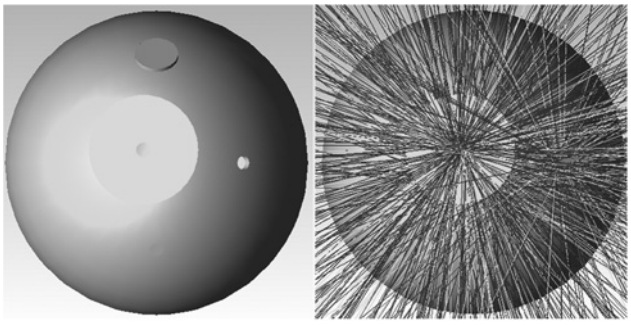

Fig. 5 *Corrective optical model*

The specific correction course is as follows:

(i) The reference beam should be passed through the input port (B) entirely and hit the integrating sphere wall at the same place like the measurement beam.

(ii) Fix the reference beam and move the measured main aperture step by step. Record the radiant flux ($P^*_{i,j}$) responded by the integrating sphere detector at every position and give the curve of radiant flux covered with the total measurement position of $(2n_x+1)\times(2n_y+1)$. The radiant flux curve is shown in Fig. 6. The radiant flux is $P^*_{0,0,-1}$ when the measured main aperture is in the centre. The average of the radiant flux is ($\overline{P^*}$).

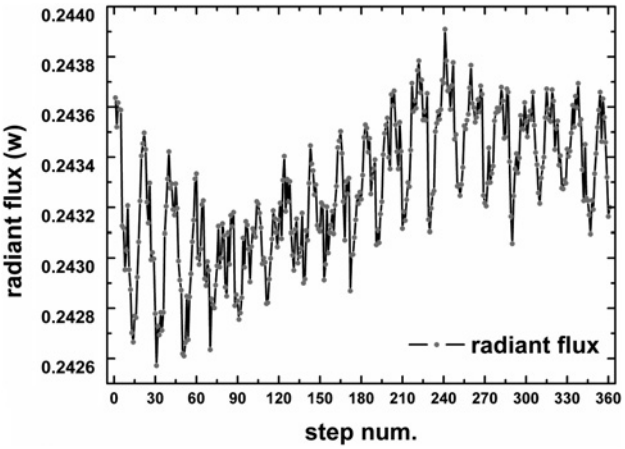

Fig. 6 *Radiant flux curve of the total measurement position*

(iii) We define that the relative change of the radiant flux is $M_{i,j}$, and it can be calculated by the equation

$$M_{i,j}=\frac{P^*_{i,j}-P^*_{0,0,-1}}{\overline{P^*}} \tag{5}$$

(iv) The curve of the relative change about the radiant flux responded by the sphere detector is shown in Fig. 7.

(v) The original experiment measurement data of the radiant flux is $P^{\mathrm{o}}_{i,j}$ and the correction data of the radiant flux can be calculated by the equation

$$P^{\mathrm{c}}_{i,j}=P^{\mathrm{o}}_{i,j}(1-M_{i,j}) \tag{6}$$

4.2 Corrections of the measurement results

A named 5 mm diameter main aperture is calibrated by a Universal Tool Measuring Microscope with a type of 19JA840087. The calibrated main aperture area is 21.12704 mm^2. Then the aperture is tested for seven times in effective area method and the aperture areas are calculated by using the original experiment measurement data and the correction data. The results are shown in Table 1. The repeatability of the uncorrected results and the corrected results within a series of repeated measurements are typically 7×10^{-5} ($n=7$), which are calculated by the standard deviation. The

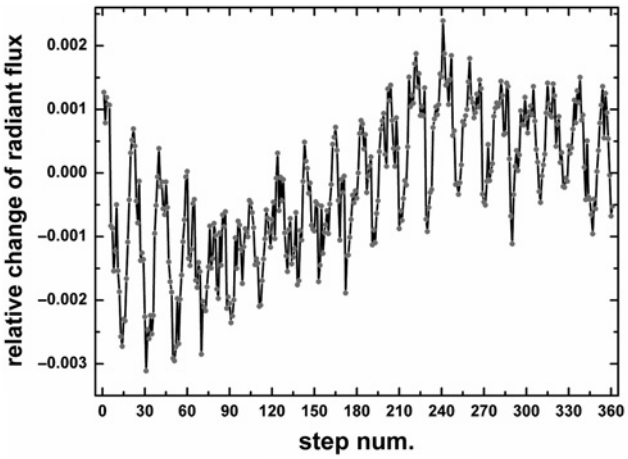

Fig. 7 *Curve of the relative change about the radiant flux*

IET Sci. Meas. Technol., 2016, Vol. 10, Iss. 2, pp. 120–123

Table 1 Results of main aperture area measurement

Aperture area	Calibrated result	Original data result	Correction data result
average value, mm^2	21.12704	21.12843	21.12435
repeatability ($n = 7$)	–	7×10^{-5}	7×10^{-5}

relative difference between the calibrated main aperture area result and the correction main aperture area result is 6.37×10^{-5}.

5 Conclusions

The corrective optical model is designed based on the real measurement optical model. Using the corrective optical model, the curve of the relative change about the radiant flux responded by the integrating sphere detector is given and the experiment measurement data are corrected. On the basis of corrective data, the corrected main aperture areas are calculated. The corrected and uncorrected main aperture area measurement results are accordant. The results prove that the optical model is a good way to correct the effect brought by the rear of the aperture serving as a part of the integrating sphere wall in effective method. The relative uncertainty of the differences between the raw results and corrected results is 9.65×10^{-5}.

The correction method is valid to improve the main aperture area measurement results. However, some deficiencies still exist in this method. The curve of the relative changes that is given by us can only correct one constant step-length aperture area measurement. If the constant step-length changed, the correction curve should be changed accordingly. To make this method more convenient with different step lengths, the relationship between the variable step length and the correction curve should be established and a lot of simulations and experiments should be carried out to justify the feasibility of the relationship and enhance the accuracy of the relationship in the future.

6 Acknowledgments

This work was supported by the National Natural Science Foundation of China (no. #41227003), by the National High-tech R&D Program (no. 2015AA123703), and by the National Natural Science Foundation of China (no. 41474161).

7 References

1 Hongrui, W., Wei, F.: 'Solar irradiance absolute radiometer with ability of automatic solar tracking', *Chin. Opt.*, 2011, **4**, (3), pp. 252–258
2 Wei, F., Bingxi, Y., Haishun, Y.: 'Solar irradiance absolute radiometer and international comparison', *Acta Opt. Sin.*, 2003, **23**, (1), pp. 112–116
3 Guangwei, Z., Xin, Y., Wei, F., *et al.*: 'Design of precise temperature control system of solar irradiance absolute radiometers', *Comput. Meas. Control*, 2012, **20**, (5), pp. 1239–1241
4 Dongjun, Y., Wei, F., Yupeng, W., *et al.*: 'Design of automatic-tracking rotating stage of solar radiometer', *Comput. Meas. Control*, 2011, **19**, (8), pp. 2001–2006
5 Dongjun, Y., Wei, F., Xin, Y., *et al.*: 'Parameters measurement of the absolute radiometer', *Comput. Meas.Control*, 2009, **17**, (10), pp. 1892–1894
6 Jiaqi, Z., Jin, Q., Wei, F., *et al.*: 'Correction of observation angle in solar radiation monitor', *Acta Opt. Sin.*, 2011, **31**, (2), p. 0212003
7 Hongrui, W., Yupeng, W., Wei, F.: 'Intelligent solar tracker with double modes', *Opt. Precis. Eng.*, 2011, **19**, (7), pp. 1605–1611
8 Baoqi, S., Xin, Y., Dongjun, Y., *et al.*: 'Precise measurement of voltages in space cryogenic radiation temperature system', *Opt. Precis. Eng.*, 2015, **23**, (7), pp. 1903–1910
9 Dongjun, Y., Wei, F., Xin, Y., *et al.*: 'Design of remote sensing signals sampling system of solar irradiance monitor', *Comput. Meas.Control*, 2009, **17**, (9), pp. 1851–1853
10 Chenghu, G., Wei, F.: 'Software design and implementation for solar irradiance monitor on FY-3A satellite', *Opt. Precis. Eng.*, 2010, **18**, (7), pp. 1476–1482
11 Bingxi, Y., Wei, F., Haishun, Y., *et al.*: 'Solar radiation measurement on shenzhou-3 spacecraft', *Chin. J. Space Sci.*, 2004, **24**, (2), pp. 119–123
12 Dongjun, Y., Wei, F., Hong, Q., *et al.*: 'On-orbit data calibration of FY-3A solar irradiance monitor', *Chin. J. Lumin.*, 2010, **31**, (5), pp. 676–681
13 Wei, F., Bingxi, Y., Yupeng, W., *et al.*: 'Solar irradiance absolute radiometers and solar irradiance measurement on spacecraft', *Chin. J. Opt. Appl. Opt.*, 2009, **2**, (1), pp. 23–28
14 Xiangzi, C., Wei, F., Yupeng, W., *et al.*: 'An overview of the method of high-precision measuring the aperture diaphragn area', *Acta Phys. Sin.*, 2013, **62**, (16), p. 164211
15 Maritoni, L., Joel, F.: 'Report on the CCPR-S2 supplementary comparison of area measurements of apertures for radiometry'. National Institute of Standards and Technology, America, 2007, pp. 50–53
16 Janjun, S., Liming, Z., Xiaobing, Z., *et al.*: 'Optical method for accurate measurement on the area of aperture diaphragm', *Infrared Laser Eng.*, 2008, **37**, (3), pp. 534–537
17 Bo, H., Xiaobing, Z., Xin, L., *et al.*: 'Technology of precise measurement of slit aperture area', *J. Atmos. Environ. Opt.*, 2011, **6**, (2), pp. 122–128
18 Stock, M., Goebel, R.: 'Practical aspects of aperture-area measurements by superposition of Gaussian laser beam', *Metrologia*, 2000, **37**, pp. 633–636
19 Ikonen, E., Toivanen, P., Lassila, A.: 'A new optical method for high-accuracy determination of aperture area', *Metrologia*, 1998, **35**, pp. 369–372
20 Lassila, A., Toivanen, P., Ikonen, E.: 'An optical method for direct determination of the radiometric aperture area at high accuracy', *Meas. Sci. Technol.*, 1997, **8**, pp. 973–977